Available online at www.sciencedirect.com
SCIENCE DIRECT®
International Journal of Heat and Fluid Flow 25 (2004) 1034–1046
International Journal of HEAT AND FLUID FLOW
www.elsevier.com/locate/ijhff

Double-diffusive natural convection in a porous enclosure partially heated from below and differentially salted

M. Bourich, M. Hasnaoui *, A. Amahmid

Department of Physics, Faculty of Sciences Semlalia, UFR TMF, BP 2390 Marrakesh, Morocco

Received 18 August 2003; accepted 21 January 2004
Available online 25 March 2004

Abstract

This paper reports numerical results of two-dimensional double-diffusive natural convection in a square porous cavity partially heated from below while its upper surface is cooled at a constant temperature. The vertical walls of the porous matrix are subjected to a horizontal concentration gradient. The parameters governing the problem are the thermal Rayleigh number ($Ra = 100$ and 200), the Lewis number ($Le = 0.1$, 1 and 10), the buoyancy ratio ($-10 \leqslant N \leqslant 10$) and the relative position of the heating element with respect to the vertical centerline of the cavity ($\delta = 0$ and 0.5). The effect of the governing parameters on fluid characteristics is analyzed. The multiplicity of solutions is explored and the existence of asymmetric bicellular flow is proved when the heated element is shifted towards a vertical boundary ($\delta = 0.5$). The solutal buoyancy forces induced by horizontal concentration gradient lead to the elimination of the multiplicity of solutions obtained in pure thermal convection when N reaches some threshold value which depends on Le and Ra.

Keywords: Heat and mass transfer; Multiplicity of solutions; Thermosolutal convection; Cross gradients of temperature and concentration; Numerical study

1. Introduction

The study of double-diffusive natural convection in fluid-saturated porous media has been motivated by its wide range of applications in many engineering fields such as evaporative cooling of high temperature systems, migration of moisture in fibrous insulation, underground disposal of nuclear wastes, spread of pollutants, drying processes, contaminant transport in saturated soils and crystal growth from liquid phase and many others. A comprehensive review of the literature concerning double-diffusive natural convection in a saturated porous media is presented in the book by Nield and Bejan (1992). The literature review indicates that most of the existing studies on double-diffusive convection are concerned with rectangular cavities where the temperature and concentration gradients are both horizontal (see for instance Trevisan and Bejan, 1986; Mamou et al., 1995; Mamou et al., 1998; Amahmid et al., 1999a,b), or vertical (see for instance Nield, 1968; Trevisan and Bejan, 1987; Murray and Chen, 1989; Chen and Chen, 1993; Amahmid et al., 1999c; Sezai and Mohamad, 1999) including different kinds of boundary conditions (constant temperature and concentration or uniform fluxes of heat and mass) and methods of solutions (the investigations are mainly conducted numerically or/and analytically).

Compared to these configurations, few investigations have considered the case where cross gradients of temperature and concentration (vertical temperature gradients and horizontal concentration gradients or vice versa) are imposed. For this kind of boundary conditions, numerical simulations of thermosolutal natural convection in a horizontal porous cavity were reported by Mohamad and Bennacer (2001). In their study, the porous matrix is heated and cooled along the vertical walls while concentration gradients are imposed vertically. The attention was paid to identify the flow regimes in the case of thermal and solutal dominating flows. It was found that multiple solutions are possible for

* Corresponding author.
E-mail address: hasnaoui@ucam.ac.ma (M. Hasnaoui).

0142-727X/$ - see front matter © 2004 Elsevier Inc. All rights reserved.
doi:10.1016/j.ijheatfluidflow.2004.01.003

Nomenclature

ABF	asymmetric bicellular flow
BAF	bicellular anti-natural flow
BNF	bicellular natural flow
D	effective dispersion coefficient (m^2/s)
d'	length of the heating source (m)
g	acceleration due to gravity (m/s^2)
H'	height of the porous cavity (m)
K	permeability of the porous medium (m^2)
k_e	thermal conductivity of the saturated porous medium (W/m^2 K)
L'	length of the porous cavity (m)
Le	Lewis number, α/D (dimensionless)
MAF	monocellular anti-natural flow
MCF	monocellular clockwise flow
MNF	monocellular natural flow
MTF	monocellular trigonometric flow
N	buoyancy ratio, $\beta_S\Delta S'/(\beta_T\Delta T')$ (dimensionless)
Nu	Nusselt number, $\int_0^1(\partial T/\partial y)_{y=1}\mathrm{d}x$ (dimensionless)
Ra	thermal Darcy–Rayleigh number, $g\beta_T K\Delta T'H'/(\alpha\nu)$ (dimensionless)
S	dimensionless solute concentration, $(S'-S'_L)/\Delta S'$
S'_L	dimensional concentration on the left wall (kg/m^3)
S'_R	dimensional concentration on the right wall (kg/m^3)
$\Delta S'$	concentration difference, $S'_R - S'_L$ (kg/m^3)
Sh	Sherwood number, $\int_0^1(\partial S/\partial x)_{x=1}\mathrm{d}y$ (dimensionless)
t	dimensionless time, $t'\alpha/(\sigma H'^2)$
T	dimensionless temperature
T'_C	dimensional temperature of the cold wall (K)
T'_H	dimensional temperature of the heating element (K)
$\Delta T'$	temperature difference, $T'_H - T'_C$ (K)
u	dimensionless horizontal velocity, $u'H'/\alpha$
v	dimensionless vertical velocity, $v'H'/\alpha$
x	dimensionless distance on x axis
y	dimensionless distance on y axis

Greeks

α	thermal diffusivity of the porous medium, $k_e/(\rho C)_f$ (m^2/s)
β_S	solutal expansion coefficient (m^3/kg)
β_T	thermal expansion coefficient (1/K)
δ'	position of the heating element (m)
δ	dimensionless position of the heating element, $2\delta'/L'$
ε	normalized porosity of the porous medium, ϕ/σ (dimensionless)
ν	kinematic viscosity of the fluid (m^2/s)
ρ	density of the fluid mixture (kg/m^3)
$(\rho C)_f$	heat capacity of the fluid (W/K)
$(\rho C)_p$	heat capacity of the saturated porous medium (W/K)
σ	heat capacity ratio, $(\rho C)_p/(\rho C)_f$ (dimensionless)
ϕ	porosity of the porous medium (dimensionless)
ψ	dimensionless stream function

Subscripts

CR	critical value
ext	extremum value
max	maximum value
min	minimum value

Superscript

$'$	dimensional variables

$Gr_m = 1000$ (modified Grashof number) and $0.8 \leqslant N \leqslant 1$. In this range of N, bifurcation from monocellular dominating flow to bicellular dominating flow is observed. Also, in the case of thermally driven flow, the concentration gradient reversal was possible. Bennacer et al. (2001) explored the stability of the same problem where oscillatory flow is predicted for a limited range of buoyancy ratios. Analytical and numerical study of double-diffusive natural convection within a horizontal porous layer, where the short vertical walls and the long horizontal ones are submitted respectively to uniform heat and mass fluxes, was conducted by Kalla et al. (2001). The existence of multiple steady-state solutions, for a given set of the governing parameters, was demonstrated. Mohamad and Bennacer (2002) studied numerically two- and three-dimensional thermosolutal convection in a horizontal enclosure filled with a saturated porous medium and submitted to cross gradients of temperature and concentration. The enclosure is differentially heated and stably stratified species concentration is imposed vertically. They demonstrated that the two-dimensional model is generally sufficient to properly model the heat and mass transfer for the ranges of investigated parameters.

The specific geometry and boundary conditions studied in this paper may be related to geothermal systems (Horne and O'Sullivan, 1974) and geologic repository for the storage of high-level radioactive wastes (Bishop and Hollister, 1974). For example, near the liquid fuel storage tanks, fuel migrates in the soil and the

convective motion induced by heating source, located in the vicinity of the tank, may reduce safety measures of the storage systems. The main objective of the present study is to introduce a horizontal concentration gradient as a disturbance to examine its effect on the multiple solutions obtained for pure thermal convection within a square enclosure locally heated from below (Robillard et al., 1988). Note that the multiplicity of solutions is not merely theoretical; its experimental evidence, for at least two different stably convective flows, was reported by Acosta and Manero (1984). Here, half of the lower boundary is heated; the heating element is either centrally located or shifted towards one of the two vertical boundaries. The results obtained show that the multiplicity of solutions vanishes when the buoyancy ratio N exceeds a critical value which depends on the other governing parameters.

2. Mathematical formulation

The studied configuration, depicted in Fig. 1, is a square-saturated porous cavity of length L' and height H'. It is assumed that the third dimension of the cavity is large enough so that the fluid flow and heat and mass transfer can be considered two-dimensional. The porous cavity is isothermally heated from below with a heating portion of length $d' = L'/2$, while the upper surface is cooled at a constant temperature. The vertical surfaces of the cavity are subjected to uniform but different concentrations. The top and bottom walls of the enclosure are impermeable to the transfer of solute, while the vertical walls and the non-heated portion of the lower surface are thermally insulated. The distance between the center of the heated element and the vertical centerline of the cavity is δ'; such that when $\delta' = 0$ the heat source is centrally located at the bottom surface. In this study, the main usual hypotheses of incompressible and laminar flow are considered. The saturated porous medium is assumed isotropic and homogeneous and its thermophysical properties are constant. Soret and Dufour effects are neglected and the Darcy model with the Boussinesq approximation are adopted in the analysis.

The following dimensionless variables are used

$$(x,y) = \frac{(x',y')}{H'}, \quad (u,v) = \frac{(u',v')}{\alpha/H'},$$

$$T = \frac{T' - T'_C}{\Delta T'}, \quad S = \frac{S' - S'_L}{\Delta S'} \quad \text{and} \quad \psi = \frac{\psi'}{\alpha} \tag{1}$$

The dimensionless governing equations based on the above definitions are as follows:

$$u = -\frac{\partial \psi}{\partial y}, \quad v = \frac{\partial \psi}{\partial x} \tag{2}$$

$$\nabla^2 \psi = Ra\left[\frac{\partial T}{\partial x} + N\frac{\partial S}{\partial x}\right] \tag{3}$$

$$\nabla^2 T = \frac{\partial T}{\partial t} + \frac{\partial (uT)}{\partial x} + \frac{\partial (vT)}{\partial y} \tag{4}$$

$$\frac{\nabla^2 S}{Le} = \varepsilon\frac{\partial S}{\partial t} + \frac{\partial (uS)}{\partial x} + \frac{\partial (vS)}{\partial y} \tag{5}$$

where ψ, T and S are the dimensionless stream function, temperature and concentration, respectively.

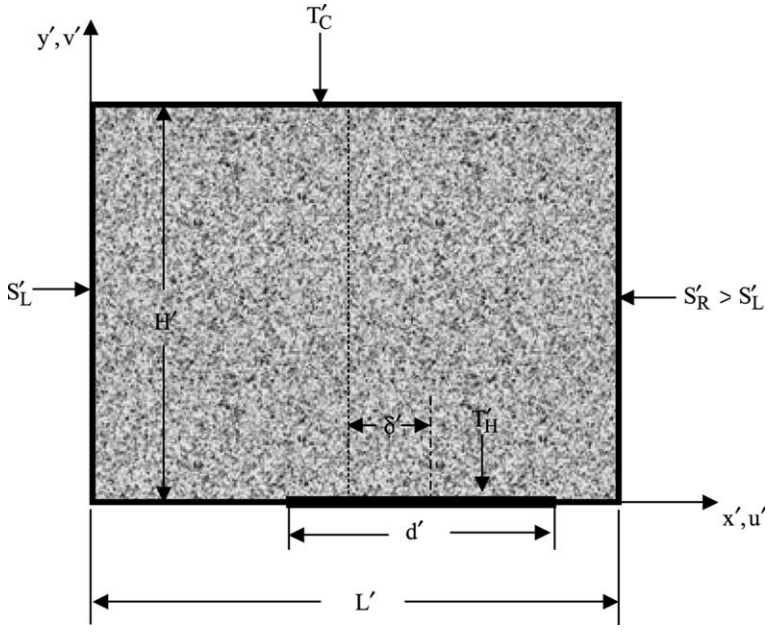

Fig. 1. Schematic of the studied configuration and coordinates system.

The dimensionless boundary conditions are:

$$\text{For } x = 0: \quad \psi = 0; \quad \frac{\partial T}{\partial x} = 0; \quad S = 0$$

$$\text{For } x = 1: \quad \psi = 0; \quad \frac{\partial T}{\partial x} = 0; \quad S = 1$$

$$\text{For } y = 0: \quad \psi = 0; \quad \frac{\partial S}{\partial y} = 0; \quad T = 1$$

$$\text{on the heated element and } \frac{\partial T}{\partial y} = 0 \text{ elsewhere}$$

$$\text{For } y = 1: \quad \psi = 0; \quad \frac{\partial S}{\partial y} = 0; \quad T = 0 \tag{6}$$

Eqs. (2)–(6) indicate that the present problem is governed by four dimensionless parameters, namely, the thermal Darcy–Rayleigh number, Ra, the buoyancy ratio, N, the Lewis number, Le, and the dimensionless position, δ, of the heating element. These parameters are defined as

$$Ra = \frac{g\beta_T K \Delta T' H'}{\alpha \nu}, \quad N = \frac{\beta_S \Delta S'}{\beta_T \Delta T'}, \quad Le = \frac{\alpha}{D}, \quad \text{and}$$

$$\delta = \frac{2\delta'}{L'} \tag{7}$$

The average values of Nusselt and Sherwood numbers, evaluated respectively on the horizontal and vertical walls, are given by

$$Nu = \int_0^1 \left.\frac{\partial T}{\partial y}\right|_{y=1} \mathrm{d}x \quad \text{and} \quad Sh = \int_0^1 \left.\frac{\partial S}{\partial x}\right|_{x=0} \mathrm{d}y \tag{8}$$

3. Numerical method

The governing equations are discretized according to the central finite difference scheme. The iterative procedure is performed using the alternating direction implicit method (ADI). The stream function field is calculated from Eq. (3) via a successive over-relaxation method (SOR). Variations by less than 10^{-5} over all grid points for the stream function was adopted as a convergence criterion. A uniform grid of 101×101 was used and the accuracy of the code was checked in pure thermal convection using the results reported in the reference by Robillard et al. (1988). It is seen, from Tables 1 and 2, that the maximum relative difference is less than 2%. The thermal and solutal boundary conditions are modified to reproduce the results reported by Goyeau et al. (1996) in the case of double-diffusive convection within a square porous enclosure differentially heated and salted. Good agreement can be seen from Table 3 with maximum deviation of about 2%.

4. Results and discussion

In the studied configuration, multiple steady-state solutions are possible. In the case of a cavity centrally heated, monocellular trigonometric/(clockwise) flow and symmetric bicellular natural/(anti-natural) flow, denoted respectively MTF/(MCF) and BNF/(BAF), are obtained. When the right half of the cavity is heated, three solutions are possible, namely, monocellular natural/

Table 1
Validation of the numerical code, for $N = 0$, in terms of stream function and Nusselt number corresponding to monocellular flow

Type of flow	δ	d'/L'	Ra	ψ_{max}/ψ_{min}		Nu	
				Present code	Robillard et al. (1988)	Present code	Robillard et al. (1988)
MTF	0	0.4	200	−8.688	−8.705	3.366	3.373
		1	100	−5.364	−5.333	2.648	2.7
			200	−8.934	−8.942	3.819	3.801
MNF	0.5	0.5	100	−5.366	−5.364	2.426	2.424
			200	−8.707	−8.666	3.496	3.505
MAF			100	4.335	4.333	1.865	1.878
			200	7.784	7.777	2.717	2.777

Table 2
Validation of the numerical code, for $N = 0$ and $\delta = 0$, in terms of extremum stream function and Nusselt number corresponding to BNF and BAF

d'/L'	Type of flow	Ra	ψ_{ext}		Nu	
			Present code	Robillard et al. (1988)	Present study	Robillard et al. (1988)
0.4	BNF	200	±5.604	±5.598	3.512	3.482
	BAF	200	±4.421	±4.474	2.341	2.347
1	BNF and BAF	100	±2.789	±2.782	2.130	2.107
		200	±5.985	±5.982	4.033	4.107

Table 3
Validation of the numerical code in the case of double-diffusive convection in a square porous cavity differentially heated and salted for $N = 0$

Ra	*Le*	Present code		Goyeau et al. (1996)	
		Nu	*Sh*	*Nu*	*Sh*
100	10	3.11	13.27	3.11	13.25
	20	3.11	19.02	3.11	18.89
200	10	4.96	20.02	4.96	19.86
	20	4.96	28.37	4.96	28.17
500	10	9.075	33.27	8.93	33.27
	20	9.075	45.91	8.93	46.77
1000	10	13.76	47.4	13.47	48.32
	20	13.76	66.95	13.47	67.45

(anti-natural) flow and asymmetric bicellular flow, denoted respectively MNF/(MAF) and ABF. It should be noted that monocellular and bicellular flows were obtained using appropriate initial conditions (for more details, see the reference by Robillard et al. (1988)). It should be mentioned that, in the case of a cavity centrally heated from below, the behaviors exhibited by the counterclockwise/(clockwise) flow when $N < 0$ are similar to those observed for clockwise/(counterclockwise) flow when $N > 0$. In addition, for the bicellular flow, the two cells exchange just their roles when the sign of N is inverted. So, only the results corresponding to positive values of N ($N > 0$) are presented for these cases. However, by changing the sign of the buoyancy ratio N, the flow structure exhibits different behaviors in the case where the heating element is shifted towards the right or the left half of the bottom wall. Thus, both positive and negative values of N are considered for the last situation (case of $\delta = 0.5$). The effect of N on flow structure and heat and mass transfer rates, corresponding to different steady-state solutions, is discussed for $\varepsilon = 1$, $Ra = 100$ and 200, $Le = 0.1$, 1 and 10, and $\delta = 0$ and 0.5. Note that numerous numerical tests were also conducted with other values of ε ($\varepsilon < 1$). It was found that this parameter does not affect neither the critical values of N nor the qualitative behavior of the unsteady phenomena. The results are presented in terms of streamlines, temperature and concentration lines and Nusselt and Sherwood numbers for the different solutions previously mentioned.

4.1. Case of a cavity centrally heated from below ($\delta = 0$)

4.1.1. Streamlines, isotherms and concentration lines

4.1.1.1. Monocellular trigonometric flow (MTF). Fig. 2(a) and (b) shows streamlines, isotherms and concentration lines corresponding to monocellular trigonometric flow obtained for $Ra = 200$, $Le = 10$ and $N = 0$ and 10. When the value of N is increased from 0 to 10, the intensity of the flow is notably enhanced since thermal and solutal buoyancy forces are cooperative in the case of MTF. The concentration field, obtained for $N = 10$, shows the presence of solutal boundary layers near the vertical walls and vertical stratification of the concentration in the core region. In the case of the temperature field, it is seen that there is a tendency to the development of thermal boundary layers. For lower values of Le, it is found that an increase of N (from 0 to 10) induces distinct thermal boundary layers in the vicinity of the thermally active surfaces and the horizontal concentration gradient is more important in the central part of the cavity. Also, it is noted that, the lower the value of Le, the more important is the increase of the flow intensity (results not presented here).

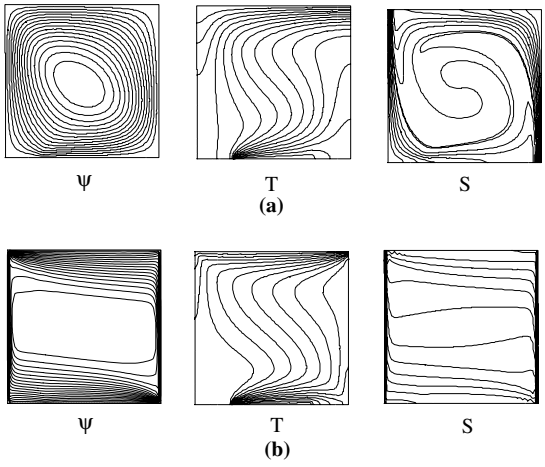

Fig. 2. Streamlines, isotherms and concentration lines corresponding to monocellular trigonometric flow for $Ra = 200$, $Le = 10$, $\delta = 0$: (a) $N = 0$ and (b) $N = 10$.

4.1.1.2. Monocellular clockwise flow (MCF). For this type of solution, the thermal and solutal buoyancy forces have opposing effects for $N > 0$ which indicates that an increase of N is not favorable to the clockwise circulation. Thus, when N is increased progressively starting from 0, the MCF transits towards the MTF when the buoyancy ratio N reaches a critical value, N_{CR}

(which depends on *Le*). In fact, when a clockwise flow, obtained for a value of N, immediately lower than N_{CR}, is used as initial condition, the transition of the MCF (characterized by $\psi_{max} > 0$ and $\psi_{min} = 0$) towards the MTF (characterized by $\psi_{max} = 0$ and $\psi_{min} < 0$) can be direct or in cascade and this, depending on R_T. The transition in cascade occurs first towards a bicellular ascending flow (BNF) at some critical value of N, then from the BNF towards the MTF when another critical value of N is reached. The critical values of N, for which the MCF disappears are presented in Tables 4 and 5 for typical values of *Le* and *Ra*. These tables show that, generally, the destruction of the MCF is precipitated (N_{CR} decreases) by increasing *Le* or *Ra*.

4.1.1.3. Bicellular natural and anti-natural flows (BNF and BAF). The effect of solutal buoyancy forces on BNF is illustrated in Fig. 3(a)–(c) for $Ra = 200$, $Le = 10$ and typical values of N (lower than that leading to the destruction of BNF). Three regions of important concentration gradients can be observed from these figures. Two of these regions are located in the vicinity of the upper parts of the vertical walls where the cells exchange important quantity of solute with these boundaries. The third region is located in the lower central part of the enclosure, in the interface between the cells where the solute exchange is by diffusion. In addition, it is seen that the increase of N engenders a decrease of the size and intensity of the right cell (i.e. the clockwise rotating cell) in favor of the left one leading to a destruction of the flow symmetry and to a displacement of the interface between the cells towards the right vertical boundary.

Table 4
Values of N_{CR} for clockwise and bicellular natural solutions for $Ra = 100$ and $\delta = 0$

Lewis number	Type of solutions			
	MCF		BNF	
	Transition towards	N_{CR}	Transition towards	N_{CR}
0.1		0.148		0.04
1	MTF	0.138	MTF	0.041
10		0.11		0.039

Note also that $\psi_{max}/|\psi_{min}|$ is reduced/(increased) by about 47%/(21%) when N passes from 0 to 0.181. These significant changes in the flow structure do not affect considerably the temperature distribution for $Le = 10$. When N reaches the critical value $N_{CR} = 0.182$, a transition from the asymmetric BNF towards MCF occurs. Similar behaviors are observed for lower values of Le, except that the concentration field is more and more dominated by diffusion as this parameter is decreased. In the case of BAF (not obtained for $Ra = 100$), the clockwise cell is located in the left part of the cavity. Also, for this type of solution, an increase of N leads to a destruction of the flow symmetry, characterized by a diminution of the size and intensity of the positive cell until the transition of the BAF towards the MTF occurs (results not presented). The critical values of N, marking the disappearance of the BNF and BAF, are presented in Tables 4 and 5 for different values of *Le*.

4.1.2. Heat and mass transfer

4.1.2.1. Case of Ra = 100. It was mentioned before that the BAF does not exist for $Ra = 100$ in the case of a cavity centrally heated from below. The effect of N on *Nu* and *Sh*, corresponding to the other solutions, is illustrated in Fig. 4(a) and (b) for $Ra = 100$ and $Le = 10$. It can be seen from this figure that *Nu* and *Sh* corresponding to MTF increase monotonically with N since solutal and thermal buoyancy forces are cooperative while important reductions of these quantities are observed in the case of MCF before the transition occurs. Quantitatively, *Nu* and *Sh* corresponding to MCF are respectively reduced by about 7.6% and 25% for $Le = 10$ when N is increased from 0 to $N_{CR} = 0.11$. In the case of BNF, the variations of *Nu* and *Sh* are limited since this type of solution is maintained only in a very small range of N. In addition, both MCF and BNF induce lower heat and mass transfer in comparison with those generated by MTF. For instance, for $Le = 10$ and $N = 0.03$, *Nu* and *Sh*, corresponding to MCF/(BNF), are respectively 1.5%/(22%) and 7%/(47%) lower than those corresponding to MTF. It is to note that the increase, with N, of *Nu*/(*Sh*) corresponding to MTF is more important for weaker/(higher) values of *Le* (results not presented). In fact, the decrease of *Le* induces an increase of the solutal boundary layer thickness (*Sh* decreases) and

Table 5
Values of N_{CR} for clockwise and bicellular solutions for $Ra = 200$, and $\delta = 0$

Lewis number	Type of solutions					
	MCF		BNF		BAF	
	Transition towards	N_{CR}	Transition towards	N_{CR}	Transition towards	N_{CR}
0.1		0.107		0.191		0.077
1	BNF	0.087	MTF	0.201	MTF	0.145
10		0.057		0.182		0.052

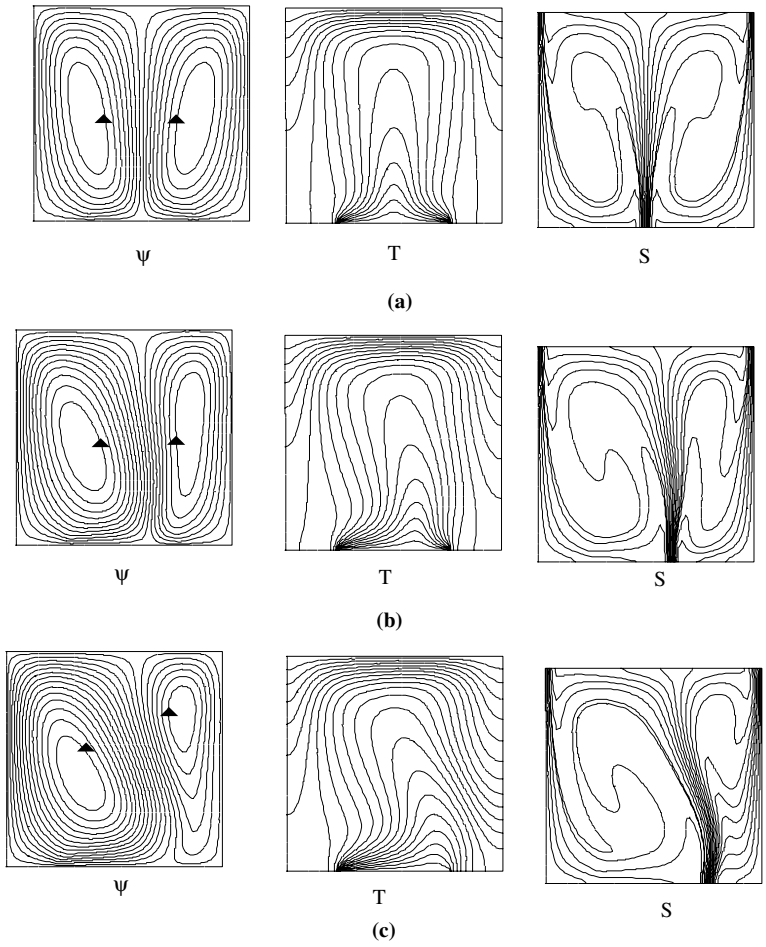

Fig. 3. Streamlines, isotherms and concentration lines corresponding to bicellular natural flow evolution with N for $Ra = 100$, $Le = 10$, $\delta = 0$ and different N: (a) $N = 0$, (b) $N = 0.1$ and (c) $N = 0.181$.

engenders an increase of the flow intensity which leads to an increase of Nu. For example, when N passes from 0 to 2, Nu/(Sh) corresponding to MTF increases by about 145%/(37%), 50%/(128%) and 1.2%/(230%) for $Le = 0.1$, 1 and 10, respectively.

4.1.2.2. Case of Ra = 200. For $Ra = 200$, both bicellular natural and anti-natural flows exist but they lead to different behaviors as shown in Fig. 5(a) and (b) for $Le = 10$. The variations of Nu and Sh with N are qualitatively similar to those described for $Ra = 100$ in the case of MTF, while the behavior exhibited by the MCF is different. In fact, for this value of Ra, the transition from MCF to MTF is in cascade; first towards BNF then from the latter towards MTF. This behavior is a consequence of the delay in the disappearance of the BNF with respect to the MCF for $Ra = 200$. The best heat transfer is induced by the BNF at relatively small values of N, but there exists a value of this parameter above which the heat transfer induced by the BNF becomes lower than that corresponding to the MTF. For $Le = 10$, Nu corresponding to the BNF is about 7%/(17.7%) higher/(lower) than the one resulting from the MTF at $N = 0$/($N_{CR} = 0.182$). Note that, in the case of $Ra = 100$, the lowest heat transfer is always induced by the BNF. The lowest heat and mass transfer are those corresponding to the BAF (the first solution which transits towards the MTF). This transition is accompanied by important increases of Nu and Sh which are respectively of about 44.8% and 120%, for $Le = 10$. The considerable reduction of Sh, observed in the case of the bicellular solutions, is mainly due to the flow structure which prevents the fluid circulation from the left vertical wall to the right vertical one (i.e. from the most salted wall to the least salted one). In fact, the interface between the two flow cells plays a resistant role to the mass transfer in the horizontal direction. The critical values of N, characterizing the different transitions obtained for $Ra = 200$, are presented in Table 5 where it is seen that the range of N for which the BAF is maintained is smaller than the one corresponding to the existence of the BNF.

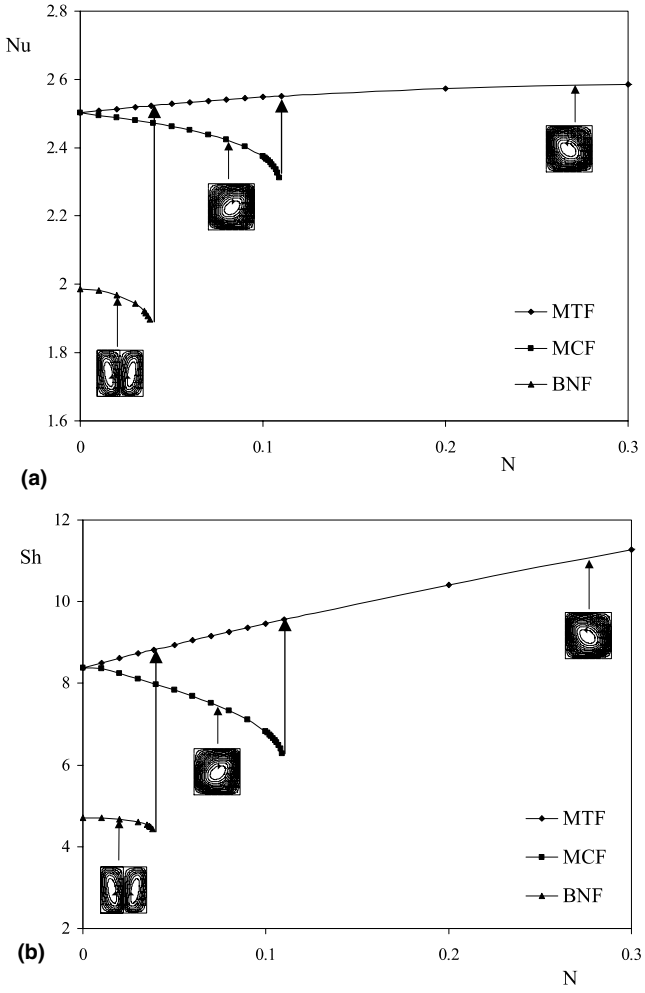

Fig. 4. Effect of N on (a) Nu and (b) Sh for $Ra = 100$, $Le = 10$, $\delta = 0$ and different solutions.

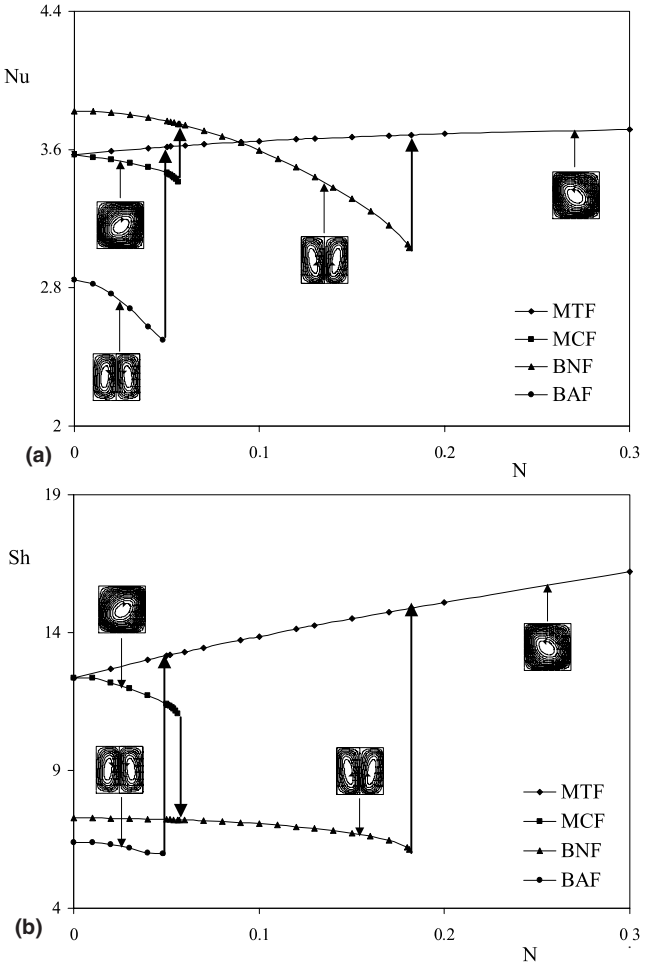

Fig. 5. Effect of N on (a) Nu and (b) Sh for $Ra = 200$, $Le = 10$, $\delta = 0$ and different solutions.

4.2. Case where the cavity is heated from the right half of the bottom ($\delta = 0.5$)

In this section the effect of the buoyancy ratio on the multiplicity of solutions, developed in a square porous cavity, heated from the right half of the bottom boundary, is examined. Before the discussion of the results obtained for this case, it is useful to point out that the results corresponding to the case where the left half of the lower boundary is heated can be deduced from those corresponding to the case where the right half of this boundary is heated. However, due to the asymmetric nature of the heating, the results of $N < 0$ cannot be deduced from those corresponding to $N > 0$. Then both positive and negative values of N will be explored here. In addition, according to the definition given in the reference by Robillard et al. (1988), the counterclockwise and clockwise flows are called monocellular natural flow (MNF) and monocellular anti-natural flow (MAF), respectively.

4.2.1. Streamlines, isotherms and concentration lines

4.2.1.1. Monocellular natural flow (MNF). Fig. 6(a)–(d) shows that the qualitative behavior of the MNF is not very different from that obtained in the case of a cavity centrally heated. In fact, the direction of the cell rotation is maintained when N is increased from 0 and the solutal and thermal boundary layers develop in the vicinity of the active surfaces (i.e. heated or salted) depending on the values of Ra, N and Le. The flow and concentration fields of Fig. 6(a)–(d) are very similar to those of Fig. 2(a)–(d), while the temperature field undergoes some modifications due to the asymmetric nature of the heating. For $N < 0$, the solutal buoyancy forces tend to induce a clockwise circulation. In fact, for $Ra = 100$, the flow intensity is decreased by decreasing N below 0 ($|N|$ increases), and the MNF transits towards the MAF when a critical value of N is reached. In the case of $Ra = 200$, the transition of the MNF occurs in cascade when N is decreased from 0; first towards the asymmetric bicellular flow (ABF) then from the latter towards the MAF. The values of N characterizing the

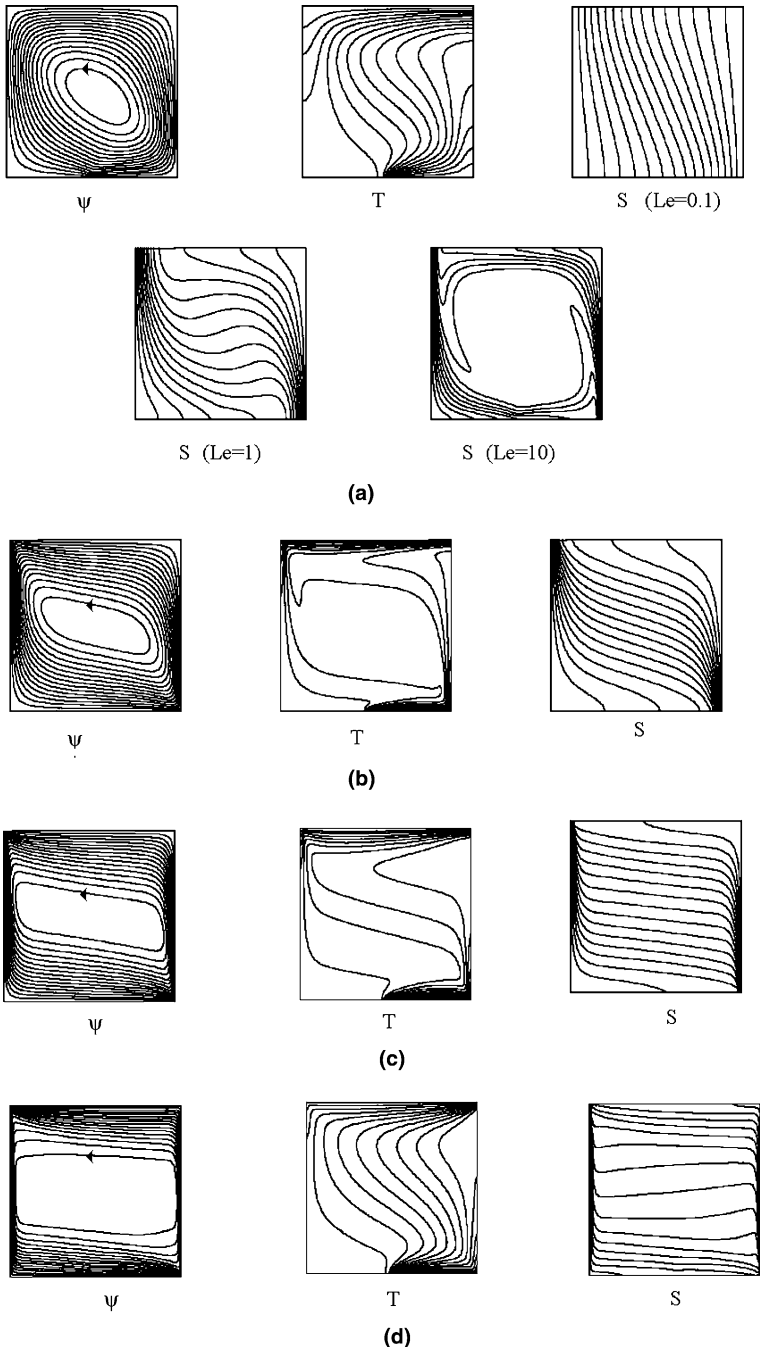

Fig. 6. Streamlines, isotherms and concentration lines corresponding to monocellular natural flow for $Ra = 200$, $\delta = 0.5$: (a) $N = 0$ and various Le; (b) $N = 10$, $Le = 0.1$; (c) $N = 10$, $Le = 1$; (d) $N = 10$, $Le = 10$.

different transitions are reported in Tables 6 and 7 for $Ra = 100$ and 200, respectively.

4.2.1.2. Monocellular anti-natural flow (MAF). Contrarily to the MNF, which disappears for $N < 0$ when this parameter reaches some threshold, the MAF is maintained because it is favored by the solutal buoyancy forces in the case of negative value of N. But for positive values of this parameter ($N > 0$), the solutal buoyancy forces are opposed to the MAF, which compels the

Table 6
Values of N_{CR} for monocellular natural and anti-natural solutions for $Ra = 100$ and $\delta = 0.5$

Lewis number	Type of solutions			
	MAF		MNF	
	Transition towards	N_{CR}	Transition towards	N_{CR}
0.1		0.074		−0.246
1	MNF	0.072	MAF	−0.278
10		0.064		−0.205

Table 7
Values of N_{CR} for monocellular (natural, anti-natural) and asymmetric bicellular solutions for $Ra = 200$ and $\delta = 0.5$

Lewis number	Type of solutions							
	MAF		MNF		ABF			
	Transition towards	N_{CR}	Transition towards	N_{CR}	Transition towards	N_{CR}	Transition towards	N_{CR}
0.1	MNF	0.074	ABF	−0.15	MNF	0.062	MAF	−0.216
1	ABF	0.058	ABF	−0.154	MNF	0.064	MAF	−0.233
10	ABF	0.043	ABF	−0.097	MNF	0.056	MAF	−0.208

latter to transit towards the MNF when N exceeds some critical value. The nature of this transition depends on both Rayleigh and Lewis numbers. In fact, for $Ra = 100$, the transition from MAF to MNF is direct independently of the Lewis number. The critical values of N, characterizing the transition from MAF to MNF, are reported in Table 6 for $Ra = 100$ and different Le. For this case ($Ra = 100$), the transition from MAF to MNF being retarded as Le increases. However, for $Ra = 200$, the transition from MAF to MNF, when the value of N is increased from 0, is direct for $Le = 0.1$ but it is in cascade for $Le = 1$ and 10. In fact, for the latter cases, the transition occurs first towards an asymmetric bicellular solution (see the following section) then from the latter towards the MNF. The critical values of N and the nature of the transitions, obtained for different Le, are reported in Table 7.

4.2.1.3. Asymmetric bicellular flow (ABF). When asymmetric heating conditions ($\delta \neq 0$) were considered in a previous work by Robillard et al. (1988), only monocellular flow was obtained in thermal natural convection. However, it is demonstrated in the present study that asymmetric bicellular flow is also possible. For $N = 0$, the asymmetric bicellular flow exists only when Ra exceeds some critical value, representing the lowest Rayleigh number above which the ABF is maintained. This critical value of Ra is 153.2 and it is determined numerically by gradually decreasing Ra from 200. Fig. 7(a) and (b) shows typical streamlines, isotherms and isosolutes corresponding to asymmetric bicellular flow for $Ra = 200$, $Le = 10$ and $N = 0$ and 0.055. The flow structure consists of two asymmetric cells such that the fluid motion above the heated element is ascendant. Note that, for $Ra = 200$ and $Le = 10$, all the tests performed to obtain asymmetric descending flow have not succeeded. The range of N for which the ABF is obtained is such that $-0.207 < N < 0.056$. For $N \leqslant -0.207$, the ABF transits towards the MAF while for $N \geqslant 0.056$, the transition is to the MNF. Note that the intensities of the recirculating cells of the ABF undergo considerable changes even for small variations of N. For example, by increasing N from 0 to 0.055 (value of N immediately lower than 0.056), ψ_{max} is decreased by

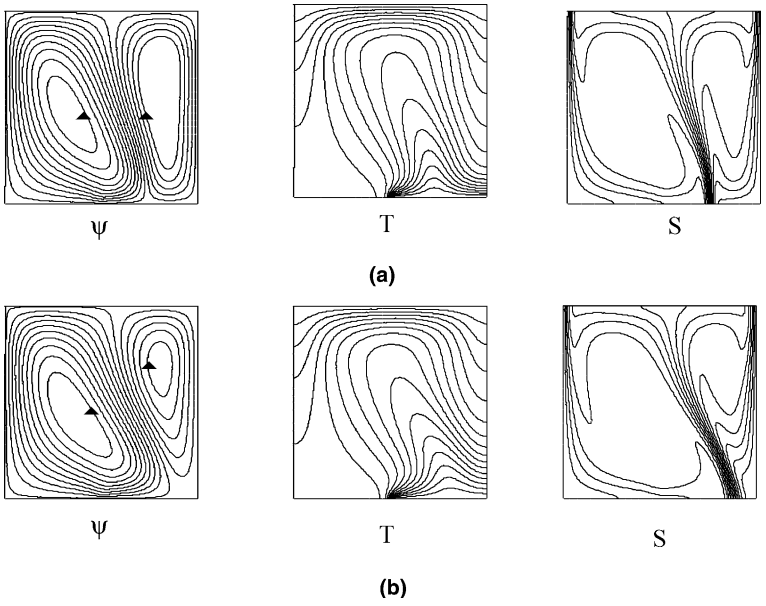

Fig. 7. Streamlines, isotherms and concentration lines corresponding to asymmetric bicellular flow evolution with N for $Ra = 200$, $Le = 10$, $\delta = 0.5$: (a) $N = 0$ and (b) $N = 0.055$.

18% while $|\psi_{min}|$ is increased by 24%. The results obtained for $Le = 1$ and $Le = 0.1$ are similar to those described for $Le = 10$, except that the critical values of N are different (see Tables 6 and 7).

4.3. Heat and mass transfer

4.3.1. Case of $Ra = 100$

The effect of N on heat and mass transfer induced by the monocellular solutions, obtained for $Ra = 100$, is illustrated in Fig. 8(a) and (b) for $Le = 10$. For positive/(negative) values of N, the thermal and solutal buoyancy forces combine their effects positively to enhance the convection in the case of MNF/(MAF). As a result, for the MNF/(MAF), the higher the buoyancy ratio $N/(-N)$ is, the higher the Nusselt and Sherwood numbers are. In addition, for positive/(negative) values of N, the solutal buoyancy forces are opposed to the MAF/(MNF), which leads to the transition of the latter towards the MNF/(MAF) as N approaches a critical value $N_{CR} = 0.063/(N_{CR} = -0.204)$. The transition from MAF/(MNF) to MNF/(MAF) leads to a decrease/(an increase) of Nu of about 38%/(6%), and to an increase of Sh of about 74%/(62%). Fig. 8(a) and (b) shows that, in the range of N, where both solutions are present, the best heat transfer is due to the MNF. While the mass transfer induced by the latter solution can be lower or higher than that of the MAF depending on the range of N. Fig. 8(a) and (b) shows clearly that the multiplicity of solutions has a considerable effect on heat and mass transfer. In fact, there are situations where the Nu induced by the MNF is 1.4 times that induced by the MAF. Similarly, the Sh induced by the MNF is about 1.7 times that of the MAF. Similar behaviors were observed for $Le = 1$ and 0.1 but are not presented here.

4.3.2. Case of $Ra = 200$

Fig. 9(a) and (b) shows the variations of Nu and Sh with N, for $Ra = 200$, $Le = 10$ and different solutions.

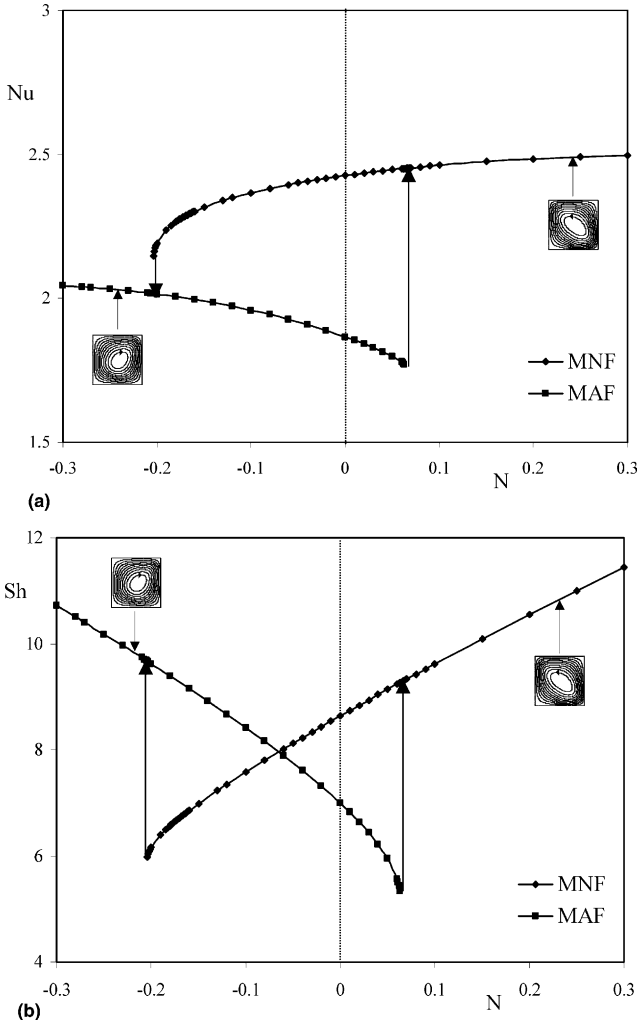

Fig. 8. Effect of N on (a) Nu and (b) Sh for $Ra = 100$, $Le = 10$, $\delta = 0.5$ and different solutions.

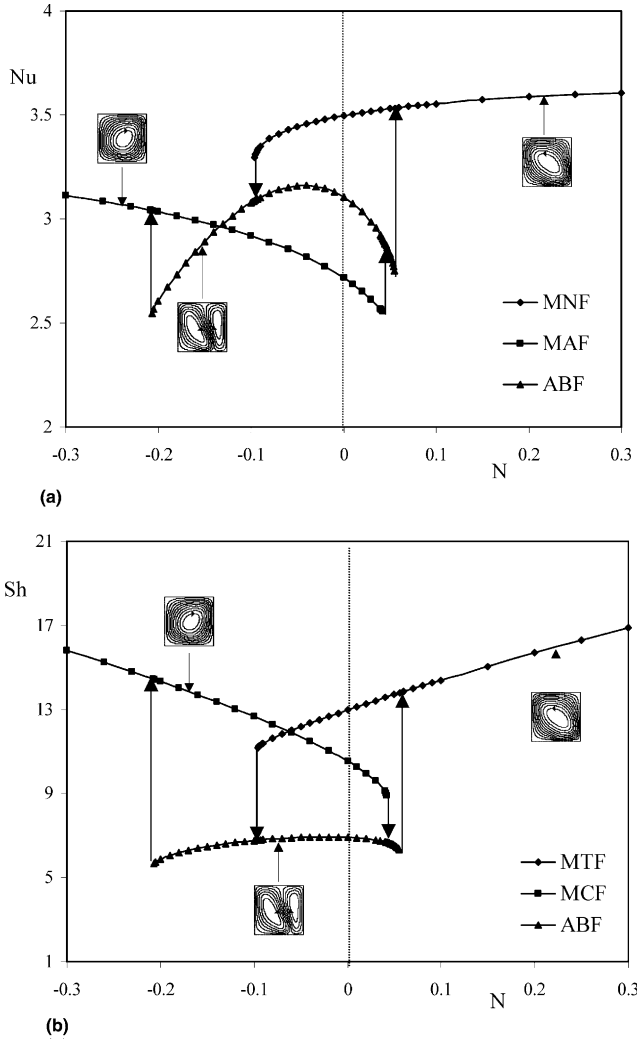

Fig. 9. Effect of N on (a) Nu and (b) Sh for $Ra = 200$, $Le = 10$, $\delta = 0.5$ and different solutions.

The behaviors exhibited by these solutions are different from those corresponding to $Ra = 100$ when N is varied, due to the presence of the asymmetric bicellular flow. In fact, by starting with the MNF/(MAF) and decreasing/(increasing) progressively N, the transition occurs first towards the ABF at $N_{CR} = -0.097/(N_{CR} = 0.043)$ then towards the MAF/(MNF) at $N_{CR} = -0.208/(N_{CR} = 0.056)$. The Nusselt number induced by the ABF goes through a maximum, at $N < 0$, when N is varied in the range where the ABF persists. In addition, there exists a range of this parameter (N) where the heat transfer induced by the ABF is higher than that corresponding to the MAF. Note that the highest heat transfer is generated by the MNF in the range where the three solutions are obtained ($-0.097 < N < 0.056$). The mass transfer induced by the ABF is almost constant (about 6.9 for $Le = 10$) and it is the lowest compared to that corresponding to the remaining solutions. For example, in the vicinity of the transition points, Sh induced by the ABF is about half that induced by the other solutions. For the MAF/(MNF), the transition is accompanied by an improvement/(a reduction) of about 13.4%/(6.4%) for *Nu* and a reduction of about 25%/(40%) in the case of *Sh*. The transition from the ABF to the MNF engenders an increase of *Nu* and *Sh* of about 28.5% and 117%, respectively, when N passes from 0.055 to 0.056. The transition from the ABF towards the MAF is accompanied by an increase of *Nu* and *Sh* of about 19.4% and 155%, respectively. A similar evolution was obtained for the different solutions for $Le = 1$ (results not presented) except that the transitions of these solutions are retarded compared to the case of $Le = 10$. However, for $Le = 0.1$ the behaviors of the different solutions are similar to those obtained for $Le = 10$ and $Le = 1$ for $N < 0$ if we except the existence of a small range of N where *Nu* induced by the MAF is higher than that induced by the MNF. For $N > 0$ and $Le = 0.1$, the behavior is different since the transition from the MAF towards the MNF takes place directly at $N_{CR} = 0.074$ as shown in Fig. 10(a) and (b).

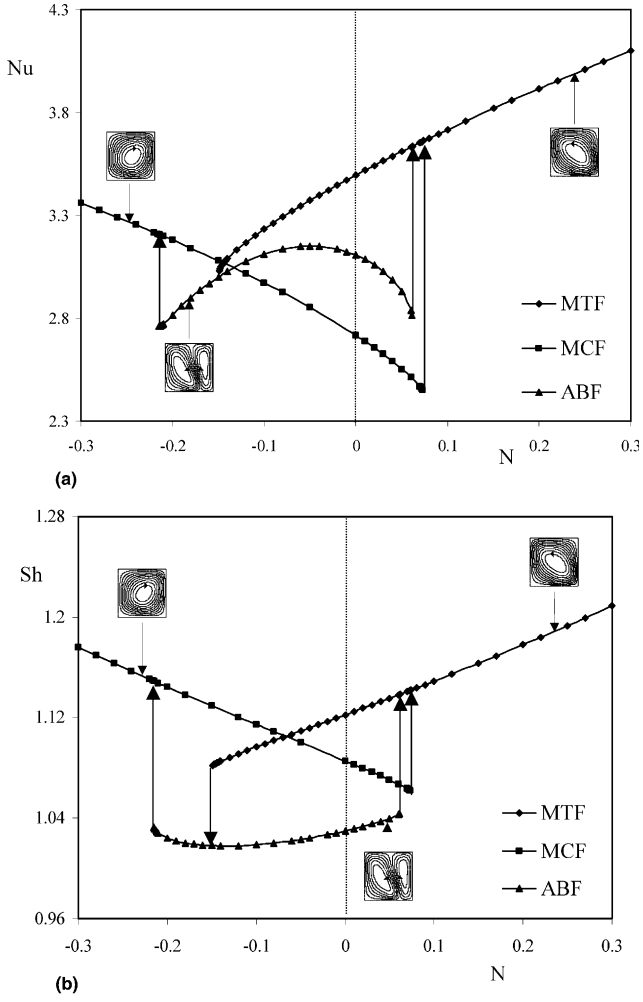

Fig. 10. Effect of N on (a) *Nu* and (b) *Sh* for $Ra = 200$, $Le = 0.1$, $\delta = 0.5$ and different solutions.

5. Conclusion

The effect of solutal buoyancy forces on the multiple steady solutions, obtained in pure thermal convection, in a porous square cavity, locally heated from below, is conducted numerically. The solutal buoyancy forces are induced by a horizontal concentration gradient imposed on the porous cavity. The main conclusions are the following:

- The effect of N on the dynamic behavior of the fluid and heat and mass transfer was found to be dependent on the type of solution, the Lewis and Rayleigh numbers, the position of the isothermal heating source.
- For a given δ, the nature of the transition from MCF($\delta = 0$)/(MAF($\delta = 0.5$)) to MTF($\delta = 0$)/(MNF($\delta = 0.5$)) depends both on *Ra* and *Le*.
- The existence of asymmetric bicellular flow is proved in the case of $\delta = 0.5$.
- The heat and mass transfer induced in the porous cavity depends on the solution considered when multiple steady states are possible. The bicellular solutions reduce considerably the heat transfer compared to the monocellular ones.
- The range of N for which a given solution is maintained depends on both *Le* and *Ra*.
- The multiplicity of solutions vanishes in the presence of horizontal solutal gradients when critical conditions are reached.

References

Acosta, R., Manero, E., 1984. Theoretical and experimental study of one and two-phase thermosyphons. Bachelor's Thesis, Facultad of Ingeniera, U.N.A.M., Mexico.

Amahmid, A., Hasnaoui, M., Vasseur, P., 1999a. Etude analytique et numérique de la convection naturelle dans une couche poreuse de Brinkman doublement diffusive. Int. J. Heat Mass Transfer 42, 2991–3005.

Amahmid, A., Hasnaoui, M., Mamou, M., Vasseur, P., 1999b. Boundary layer flows in a vertical porous enclosure induced by opposing Buoyancy Forces. Int. J. Heat Mass Transfer 42, 3599–3608.

Amahmid, A., Hasnaoui, M., Mamou, M., Vasseur, P., 1999c. Double-diffusive parallel flow induced in a horizontal Brinkman porous layer subjected to constant heat and mass fluxes: analytical and numerical studies. J. Heat Mass Transfer 35, 409–421.

Bennacer, R., Mohamad, A.A., Akrour, D., 2001. Transient natural convection in an enclosure with horizontal temperature and vertical solutal gradients. Int. J. Therm. Sci. 40, 899–910.

Bishop, W.P., Hollister, C.D., 1974. Sea-bed disposal: where to look. Nucl. Technol. 24, 425–443.

Chen, F., Chen, C.F., 1993. Double-diffusive fingering convection in a porous medium. Int. J. Heat Mass Transfer 36, 793–807.

Goyeau, A., Songbe, J.P., Gobin, D., 1996. Numerical study of double-diffusive natural convection in a porous cavity using the Darcy–Brinkman formulation. Int. J. Heat Mass Transfer 39, 1363–1378.

Horne, R.N., O'Sullivan, M.J., 1974. Oscillatory convection in a porous medium heated from below. J. Fluid Mech. 66, 339–352.

Kalla, L., Vasseur, P., Benacer, R., Beji, H., Duval, R., 2001. Double diffusive convection within a horizontal porous layer salted from the bottom and heated horizontally. Int. Comm. Heat Mass Transfer 28, 1–10.

Mamou, M., Vasseur, P., Bilgen, E., 1995. Multiple solutions for double-diffusive convection in a vertical porous enclosure. Int. J. Heat Mass Transfer 38, 1787–1798.

Mamou, M., Vasseur, P., Bilgen, E., 1998. Double diffusive convection instability in a vertical porous enclosure. J. Fluid Mech. 368, 263–289.

Mohamad, A.A., Bennacer, R., 2001. Natural convection in a confined saturated porous medium with horizontal temperature and vertical solutal gradients. Int. J. Therm. Sci. 40, 82–93.

Mohamad, A.A., Bennacer, R., 2002. Double diffusion natural convection in an enclosure filled with saturated porous medium subjected to cross gradients; stably stratified fluid. Int. J. Heat Mass Transfer 45, 3725–3740.

Murray, B.T., Chen, C.F., 1989. Double diffusive convection in a porous medium. J. Fluid Mech. 201, 147–166.

Nield, D.A., 1968. Onset of thermohaline convection in a porous medium. Water Resour. Res. 4, 553–560.

Nield, D.A., Bejan, A., 1992. Convection in Porous Media. Springer-Verlag.

Robillard, L., Wang, C.H., Vasseur, P., 1988. Multiple steady states in a confined porous medium with localized heating from below. Int. J. Heat Mass Transfer 13, 91–110.

Sezai, I., Mohamad, A.A., 1999. Three-dimensional double-diffusive convection in a porous cubic enclosure due to opposing gradients of temperature and concentration. J. Fluid Mech. 400, 333–353.

Trevisan, O.V., Bejan, A., 1986. Mass and heat transfer by natural convection in a vertical slot filled with porous medium. Int. J. Heat Mass Transfer 29, 403–415.

Trevisan, O.V., Bejan, A., 1987. Mass and heat transfer by high Rayleigh number convection in a porous medium heated from below. Int. J. Heat Mass Transfer 30, 2341–2356.